Published in final edited form as:
J Immunol. 2013 April 1; 190(7): 3541–3551. doi:10.4049/jimmunol.1202264.

A Critical Role for Toll-like Receptor-4 Induction of Autophagy in the Regulation of Enterocyte Migration and the Pathogenesis of Necrotizing Enterocolitis

Matthew D. Neal[*], **Chhinder P. Sodhi**[*], **Mitchell Dyer**[*], **Brian T. Craig**[*], **Misty Good**[†], **Hongpeng Jia**[*], **Ibrahim Yazji**[*], **Amin Afrazi**[*], **Ward M. Richardson**[*], **Donna Beer-Stolz**[‡‡], **Thomas Prindle**[*], **Zachary Grant**[*], **Maria F. Branca**[*], **John Ozolek**[‡], and **David J. Hackam**[*]

[*]Division of Pediatric Surgery, Department of Surgery, Children's Hospital of Pittsburgh and Department of Surgery, University of Pittsburgh School of Medicine

[†]Division of Newborn Medicine, Children's Hospital of Pittsburgh and Department of Pediatrics, University of Pittsburgh School of Medicine

[‡]Division of Pathology, Children's Hospital of Pittsburgh and Department of Pathology, University of Pittsburgh School of Medicine

[‡‡]Department of Cell Biology and Center for Biological Imaging, University of Pittsburgh School of Medicine

Abstract

Necrotizing enterocolitis (NEC) develops in response to elevated Toll-like receptor-4 (TLR4) signaling in the newborn intestinal epithelium, and is characterized by TLR4-mediated inhibition of enterocyte migration and reduced mucosal healing. The downstream processes by which TLR4 impairs mucosal healing remain incompletely understood. In other systems, TLR4 induces autophagy, an adaptive response to cellular stress. We now hypothesize that TLR4 induces autophagy in enterocytes, and that TLR4-induced autophagy plays a critical role in NEC development. Using mice selectively lacking TLR4 in enterocytes(TLR4$^{\Delta IEC}$), and in TLR4-deficient cultured enterocytes, we now show that TLR4 activation induces autophagy in enterocytes. Immature mouse and human intestine showed increased expression of autophagy genes compared to full-term controls, and NEC development in both mouse and human was associated with increased enterocyte autophagy. Importantly, using mice in which we selectively deleted the autophagy gene ATG7 from the intestinal epithelium (ATG7$^{\Delta IEC}$), the induction of autophagy was determined to be required for and not merely a consequence of NEC, as ATG7$^{\Delta IEC}$ mice were protected from NEC development. In defining the mechanisms involved, TLR4-induced autophagy led to impaired enterocyte migration both in vitro and in vivo, which in cultured enterocytes required the induction of RhoA-mediated stress fibers. These findings depart from current dogma in the field by identifying a unique effect of TLR4-induced autophagy within the intestinal epithelium in the pathogenesis of NEC, and identify that the negative consequences of autophagy on enterocyte migration play an essential role in its development.

Introduction

Necrotizing enterocolitis (NEC) is a devastating disease of preterm infants, and is the leading cause of death from gastrointestinal disease in neonates (1). Despite advances in the

Correspondence: David J. Hackam, MD, PhD, Division of Pediatric Surgery, Children's Hospital of Pittsburgh of UPMC, One Children's Hospital Drive, 4401 Penn Avenue, Pittsburgh, PA 15224, Tel 412 692 8449, Fax 412 692 8299, david.hackam@chp.edu.

care of premature infants overall, the overall survival of infants with NEC is unchanged since its initial description over 30 years ago (2). NEC is characterized by patchy areas of inflammation and necrosis that predominantly involve the small intestine, and is thought to develop from an uncontrolled inflammatory response to bacterial colonization of the premature intestine (3, 4). While initial studies to explain the pathogenesis of NEC have focused on various aspects of the immune system that render the premature host susceptible to intestinal inflammation, none of these approaches has yielded a unifying cause for NEC (5). By contrast, more recent studies have focused on the ability of the normal infant to adapt to the events surrounding the exposure to bacteria and their products, such as lipopolysaccharide. For instance, we (6) and others (7, 8) have identified that the receptor for lipopolysaccharide i.e. Toll Like Receptor 4 (TLR4) is elevated in the premature intestinal epithelium in humans and mice, and that excessive TLR4 signaling during this vulnerable period is required for NEC development (6, 9, 10). At the cellular and tissue levels, we (6, 11, 12) have shown that a primary event leading to NEC involves a TLR4-mediated reduction in enterocyte migration, which can significantly impairs the extent of intestinal healing, leading to bacterial translocation and sepsis (13). Importantly however, the downstream processes by which TLR4 activation leads to impaired mucosal healing remain incompletely understood (14).

One such response that is downstream of TLR4 signaling and that could play a role in the pathogenesis of NEC through regulation of migration is autophagy (15), a highly conserved process of cellular catabolism which has been shown to be active in adaptive responses to metabolic stress (16). Autophagy is characterized by the activation of ATG7 and ATG16 among other molecules leading to the transfer of LC3-1 to LC3-II which results in the formation of double membrane vesicles called autophagosomes (17). Although traditionally considered a cellular survival mechanism directed at the retrieval of membrane and energy substrates (18), recent evidence has shown that impaired autophagy has been linked to the development of intestinal inflammation, as mutation of the autophagy gene ATG16 has been identified as a risk factor for the development of Crohn's disease (19) and experimental colitis (20). More recently, a variety of studies have linked the autophagy pathway with the regulation of migration in several cell types (21–24). Studies such as these have expanded the role of autophagy beyond that of the control of individual cell survival, to a pathogenetic role that could be critical in diseases such as necrotizing enterocolitis that are characterized by impaired mucosal healing.

We now hypothesize that activation of TLR4 induces autophagy in enterocytes, and that the activation of autophagy through TLR4 plays a critical role in NEC development. In support of this hypothesis, using mice in which either TLR4 or the autophagy gene Atg7 were selectively deleted from the intestinal epithelium, we now show that TLR4 signaling within the intestinal mucosa leads to an induction of autophagy, and that the induction in autophagy is required for the development of NEC. In seeking to define how autophagy induction could lead to NEC, we further reveal that the induction of autophagy leads to an impairment in enterocyte migration through the activation of RhoA-GTP-ase. These findings depart from current dogma in the field by identifying a unique effect of TLR4-induced autophagy within the intestinal epithelium – as opposed to other cells – on the pathogenesis of necrotizing enterocolitis, and identify that the negative consequences of autophagy on enterocyte migration play an essential role in its development.

Material and Methods

Cell culture and reagents

The enterocyte line IEC-6 was obtained from the American Type Culture Collection (ATCC) and maintained as described (25). Atg16-deficient and Atg7-deficient IEC-6

enterocytes were generated by transduction of lentiviral particles (Invitrogen) containing Atg16 shRNA or Atg7 shRNA (Open Biosystems) using the four plasmid lentiviral packaging system in HEK 293 cells. Stable integration of lentivirus was obtained by selection of cells using puromycin-containing media (5μg/ml), and knockdown of Atg16 or Atg7 was verified by SDS-PAGE, q-RT-PCR and immunocytochemistry. TLR4-deficient IEC-6 enterocytes were generated as described (26). Where indicated, cells were treated with LPS (*Escherichia coli* 0111:B4 purified by gel filtration chromatography (>99% pure; Sigma-Aldrich) for 0–12hrs at a concentration of 50 μg/ml LPS which corresponds to our recent measurement of ~15–20 EU/ml as determined by *Limulus* assay, which is within the range of fecal LPS that is observed in NEC in both mice and humans (6). Cells were treated with scrambled lentivirus as described (27).

Antibodies used in this study are as follows: LC3, Atg16 - MBL International (Woburn, MA), Atg7, f-actin – Sigma; E-cadherin – R&D Systems Inc (Minneapolis, MN), sucrase isomaltase – Santa Cruz, BRDU detection kit – Pharmingen (San Jose, CA), actin (Sigma), phalloidin – Invitrogen (Grand Island, NY). The LC3 antibody was validated for immunohistochemistry as shown in Supplemental Figure 1.

Constitutively active (RhoA L63) and dominant negative RhoA (RhoA N19) adenoviruses were obtained from Cell Biolabs and infected into IEC-6 cells for 36h prior to further treatment.

For immunohistochemistry, cells were processed as described and fluorescent images were captured using either an Olympus Fluoview 1000 confocal microscope under a x60 oil immersion objective using standard filter sets. Digital images were prepared, quantified and labeled using ImageJ software. SDS-PAGE was performed as described (28).

Pull-down assay to determine RhoA activation

RhoA activation was determined in a pull-down assay as we have previously described according to the manufacturer's protocol (Cytoskeleton) (11, 12). This assay, in which Rhotekin-bound beads are incubated with cellular lysates, is based upon the finding that activated RhoA (i.e. RhoA-GTP) selectively binds to the effector molecule Rhotekin (29), while inactive RhoA (i.e. RhoA-GDP) does not. Where indicated, IEC-6 wild-type, Atg7-k/d or Atg16-k/d cells were treated with the autophagy inducer rapamycin (Calbiochem, 30nm, 30minutes), or the Rho inhibitor, soluble C3 exotoxin (Calbiochem, 0.1ug/ml, 2hr) and/or LPS (25ug/kg, 3hr). GTPγS treated lysates served as a positive control for Rho activation in all cases. Biochemical findings of RhoA activation were confirmed by immuno-histochemical techniques in which the formation of stress fibers provides a reliable marker of RhoA activation, and in which cells were imuostained with fluorescent phalloidin and examined by confocal microscopy.

Quantitative real-time PCR

Total RNA was isolated from cultured enterocytes or ileal mucosal scrapings from control and NEC mouse and human intestine using the RNeasy kit (Qiagen), and reverse transcribed (1 μg of RNA) using the QuantiTect Reverse Transcription Kit (Qiagen). Quantitative real-time PCR was performed as previously described using the Bio-Rad CFX96 Real-Time System (Biorad, Hercules, CA) using the primers described below, and are reported as fold change relative to GAPDH as a housekeeping gene:

GAPDH: Mouse: Forward: TGAAGCAGGCATCTGAGGG; Reverse: CGAAGGTGGAAGAGTGGGAG; 102bp; Human: Forward: TCTCCTCTGACTTCAACAGCGACA; reverse: CCCTGTTGCTGTAGCCAAATTCGT; 126bp.

Atg7: Human/mouse/rat: Forward: AGCCCACAGATGGAGTAGCAGTTT; Reverse: TCCCATGCCTCCTTTCTGGTTCTT; 184bp

Atg16: Human/mouse/rat: Forward: TGTCTTCAGCCCTGATGGCAGTTA; Reverse: AGCACAGCTTTGCATCCTTTGTCC; 189bp

LC3: mouse: Forward: CCGCAGCCCTTGAGCTCGAG; Reverse: GGGTGCTGGTCGCGGATCTG; 192 bp; human: forward: CCATGTCAACATGAGCGAGTTGGT; reverse: TGGGAGGCGTAGACCATATAGAGGAA; 192 bp

Beclin1: Human/mouse: Forward: TGCTCTGGCCAATAAGATGGGTCT; Reverse: GGAAAGCCACCATTGCATGGTCAA 173 bp

CxCl15 (mouse IL-8): Mouse: Forward: GCTGGGATTCACCTCAAGAA; Reverse: TCTCCGTTACTTGGGGACAC; 180bp

PCNA: mouse: Forward: AAAGATGCCGTCGGGTGAATTTGC; Reverse: AATGTTCCCATTGCCAAGCTCTCC.

Measurement of enterocyte migration in vitro and in vivo

To measure enterocyte migration *in vitro*, IEC-6, Atg7 k/d and ATG16k/d cells were grown in antibiotic-free medium in 35mm glass bottom dishes for 24hours and a confluent monolayer was formed. Cells were treated with LPS (50 μg/ml), rapamycin (30nM), chloroquine (20uM, Sigma), or soluble C3 exotoxin (01.ug/ml) for 1 h before scraping. In experiments that involved the combination of LPS with another treatment, cells were treated with the experimental compound for 30 minutes prior to exposure to LPS. In order to measure enterocyte migration, a wound was created within the confluent monolayer by scraping a layer of confluent cells with a pipet tip. Cells were then observed as they moved into the wound on the stage of a Vivaview FL Incubator and Fluorescence Microscope (Olympus) which allowed for incubation at 37°C over a 12 hour period. Static images were obtained at hourly intervals, and an identically sized region of interest overlapping the wound was selected between fixed points in the visible field which were constant for all experiments in all groups using Metamorph software (Universal Imaging Corp.). The kinetics of wound closure were then determined by identifying the movement of cells in the *x–y* plane across the regions of interest. Using Metamorph, the area of the region of interest covered by cells was calculated at each time point, and the change in area of a 24 hour period at each fixed time point was assessed. The rate of enterocyte migration was then calculated as percent wound closure as the cells migrated across the fixed region of interest.

To measure enterocyte migration *in vivo*, animals were injected with 5'-BrdU (50 mg/kg; Sigma-Aldrich) i.p. and then sacrificed 24 h later. Samples of terminal ileum were then immunostained using anti-BrdU Abs as described (30) and then counterstained with hematoxylin according to the manufacturers protocol. Enterocyte migration was determined by measuring the distance from the bottom of the crypt to the foremost labeled enterocyte and expressing the distance as a percentage of total villus height at each time point using Metamorph software.

Generation of knockout and transgenic ATG7$^{\Delta IEC}$, TLR4$^{-/-}$ and TLR4$^{\Delta IEC}$ mice

All animal studies were approved by the Institutional Review Board at the University of Pittsburgh and conducted in accordance with the guidelines set forth by the Animal Research and Care Committee at the University of Pittsburgh and the Children's Hospital of Pittsburgh of UPMC. C57Bl/6 mice were obtained from The Jackson Laboratory and housed in accordance with University of Pittsburgh animal care guidelines. TLR4$^{-/-}$ mice were generated by first generating a floxp-TLR4 mice which we then bred with the EIIa-Cre

mouse (Jackson Labs) to generate the global TLR4$^{-/-}$ mouse as we recently described (31). In order to selectively remove TLR4 from the intestinal epithelium the floxp-TLR4 mice were bred with the Villin-Cre mice (Jackson Labs) to generate an enterocyte-specific TLR4 knock-out mouse (TLR4$^{\Delta IEC}$ mice), as we have recently described (26). ATG7$^{flox/flox}$ mice were the generous gift of Dr. Tomoki Chiba (University of Tokyo). To generate intestinal epithelial-specific ATG7 conditional knockout mice (strain ATG7$^{\Delta IEC}$), (32), we bred the ATG7$^{flox/flox}$ mouse on a C57/Bl-6 background with transgenic mouse line expressing villin-cre (B6.SJLTg (Vil-cre)997Gum/J, Jackson Labs). Mice were then backcrossed seven times before use, and were shown to be deficient in Atg7, and characterized in detail as shown in Supplemental Figure 2.

Induction of experimental necrotizing enterocolitis and endotoxemia

Experimental NEC was induced in 10 day old mice as we have described (33)using a combination of formula gavage (Similac Advance infant formula (Ross Pediatrics):Esbilac canine milk replacer 2:1) five times/day, and hypoxia (5%O_2, 95%N_2) for 10min in a hypoxic chamber (Billups-Rothenberg, DelMar, CA) twice daily for 4 days. Animals are fed 50 μl/g of mouse body weight by gavage over 2–3 min, using a 24-French angiocatheter which is placed into the mouse esophagus under direct vision. Samples of the terminal ileum were harvested at day 4 for analysis. This protocol induces patchy intestinal inflammation in mice that is predominantly localized to the small bowel, and which resembles human NEC (27). Control (i.e., non-NEC) animals of all tested strains remained with their mothers and received breast milk. The severity of experimental NEC was graded by a blinded pathologist using a previously validated scoring system from 0 (normal) to 3 (severe) as previously described (27).

Where indicated, formula fed mice were treated with either rapamycin (EMD Millipore, 5mg/kg) or chloroquine (Sigma, 60mg/kg) via i.p. route once daily on each day of the NEC model, under conditions which have been shown to induce or inhibit autophagy, respectively (34, 35). All groups included a vehicle alone control in all cases (saline with 1% EtOH) alone. Endotoxemia was induced in 3 week old mice for all strains by intraperitoneal injection of LPS (5mg/kg) as previously described. After 24 hours, animals were euthanized and the terminal ileum was harvested for analysis.

Human tissue

Discarded human tissue was obtained via waiver of consent in accordance with University of Pittsburgh anatomical tissue procurement guidelines with approval from the University of Pittsburgh Institutional Review Board. In all cases, tissue was obtained from either aborted fetuses, from human infants undergoing surgical resection for the management of severe NEC, or from control infants at the time of stoma closure during which all intestinal inflammation had resolved. Control infants underwent intestinal resection and stoma closure in all cases beyond 40 weeks post-conceptual age and were thus full term at the time at which analysis was undertaken. Lysates were then purified from mucosal scrapings after irrigation of the bowel to remove luminal contents.

Electron microscopy

Samples obtained from both control and experimental groups were fixed in 2.5% gluteraldehyde for processing for electron microscopy. Scanning electron microscopy (SEM) was performed using a JEOL electron microscope, model number JSM6335F after tissues were placed into 8mm^3 blocks and post-fixed in 1% Osmium tetroxide (OsO4) in 0.1 M PBS. Following alcohol dehydration, tissues were washed with hexamethyldisilizane and mounted on studs for sectioning. For transmission electron microscopy (TEM), tissues were placed on 1mm^3 blocks and post-fixed with 1% OsO4 containing 1% potassium

ferricyanide. Following alcohol dehydration, tissues were further dehydrated with propylene oxide and then infiltrated with a 1:1 mix of propylene oxide and epon overnight. Samples were then infiltrated with pure epon overnight at 4° C, embedded in pure epon at 37° C for 24 hours, and cured for 48 hours at 60° C. Samples were 70nm sectioned on an Ultra Microtome, placed on copper grids, and stained with urinal acetate and lead citrate.

Statistical analysis

Data are means ± SEM, and comparisons are by two-tailed Student's t test or ANOVA, with statistical significance accepted for $p < 0.05$. All experiments were performed at least in triplicate. For mouse studies, at least 5 mice per group were included.

Results

TLR4 induces autophagy in intestinal epithelial cells in vitro and in vivo

We first sought to determine whether TLR4 activation could induce autophagy in enterocytes, and to then evaluate whether enterocyte autophagy may play a role in the pathogenesis of NEC. As shown in Figure 1, treatment of IEC-6 enterocytes with the TLR4 agonist lipopolysaccharide (LPS) led to a significant increase in autophagy, as demonstrated by an increase in the detection of autophagosomes within IEC-6 enterocytes by confocal microscopy using the autophagy maker LC3 (Figure 1 **panel A i–ii**), by an increase in the accumulation of double-membrane bound vesicles that resemble autophagosomes as revealed by electron microscopy (Figure 1 **panel A v–vi**), and by an increase in the ratio of LC3-II to actin as detected by SDS-PAGE (Figure 1 **panel C i–ii**). To confirm a specific role for TLR4 in enterocytes in the induction of autophagy in response to LPS stimulation, we utilized a stable line of IEC-6 cells that lack TLR4 that we had recently generated (TLR4-k/d) (26). As shown in Figure 1, TLR4-k/d cells showed no increase in autophagy in response to LPS addition, as reflected by reduced accumulation of LC3-positive vesicles (Figure 1, **panel A iii-iv**) and reduced LC3-II to actin conversion via SDS-PAGE (Figure 1 **panel C i–ii**). As an important control, depleting serum from the growth media – which is known to induce autophagy in other cells (36) – was found to increase autophagy in TLR4-k/d cells (Figure 1 **panel A vii**), confirming that the autophagy machinery in the TLR4-deficient cells is still largely intact, yet is non-responsive to LPS. In parallel experiments, we confirmed the validity of the anti-LC3 antibody by treating RAW 264.7 macrophages with rapamycin or exposing these cells to serum free media – which resulted in increased LC3 staining – then replenishing the serum, which diminished LC3 expression within the cytoplasm (Supplementary Figure 1).

To evaluate whether TLR4 activation could induce enterocyte autophagy *in vivo*, we next injected newborn mice with LPS or saline and evaluated the induction of enterocyte autophagy. As shown in Figure 1, LPS injection caused an increase in the intracellular accumulation of LC3 within the intestinal epithelium (Figure 1 **panel B i–ii**) as well as an increase in the expression of LC3-II to actin by SDS-PAGE (Figure 1 **panel D i–ii**). It is noteworthy that LPS injection caused a similar increase in the induction of autophagy as determined by SDS-PAGE in mice that were both 10 days and 21 days old (Supplemental Figure 1 panel B). Importantly, LPS injection did not induce autophagy in $TLR4^{-/-}$ mice as revealed both by confocal microscopy (Figure 1 **panel B iii-iv**) and SDS-PAGE (Figure 1 **panel D i–ii**). Taken together, these findings illustrate that TLR4 activation leads to an increase in enterocyte autophagy, both *in vitro* and *in vivo*. We next sought to evaluate the expression of autophagy genes in the intestine of premature versus full term intestine in order to evaluate the potential role of TLR4-induced enterocyte autophagy in the pathogenesis of necrotizing enterocolitis.

Autophagy genes are increased in the premature versus full term intestine in both mice and humans

In order to evaluate a potential role for TLR4-induced autophagy in the pathogenesis of NEC, we next examined the expression of critical autophagy genes in the premature versus mature intestine of both mice and humans. As shown in Figure 2 **panel A**, the expression of TLR4, as well as the expression of the autophagy genes ATG7, LC3, ATG16 and Beclin1 were significantly higher in premature versus mature mouse intestine. Importantly, this pattern was also seen in the human, as the expression of TLR4, ATG7, LC3, ATG16 and Beclin1 were significantly greater in the intestine from fetal as compared to full term subjects (Figure 2 **panel B**). These findings suggest that the molecular machinery necessary for the induction of autophagy is upregulated in the premature state, raising the possibility that the subsequent induction of autophagy may play a role in the development of necrotizing enterocolitis, a disease that predominantly favors the premature intestine.

Enterocyte autophagy occurs in mice and humans with NEC, and in mice requires TLR4 activation

We next examined whether NEC was associated with an induction in enterocyte autophagy, and if so, whether TLR4 signaling within the intestinal epithelium was required for this induction to occur. To do so, NEC was induced in newborn mice using a combination of hypoxia and formula feeding as we have previously described (27), and the degree of autophagy within the intestinal mucosa was determined by microscopic and biochemical means. As shown in Figure 3 **panel Ai**, the development of NEC in mice was associated with a significant increase in the extent of autophagy in enterocytes, as manifest by an accumulation of double membrane vesicles by electron microscopy, that were not observed in control, breast fed mice (Figure 3 **panel Aii, arrows show double membrane vesicles**). Findings of increased enterocyte autophagy in mice with NEC were also observed by confocal microscopy, in which the accumulation of LC3-positive autophagosomes were increased as compared with breast fed controls (Figure 3 **panel B i and ii**). Importantly, increased enterocyte autophagy was also observed in tissue obtained from human patients with NEC, in which an increase in the expression of LC3-positive autophagosomes was detected, as compared with control tissue that was obtained at the time of stoma closure (Figure 3 **panel C i and ii**). Intestinal tissue that had been obtained from aborted fetuses also showed a significant increase in staining for LC3 within the intestinal epithelium (Figure 3 **panel C iii**), in findings that are consistent with the results shown in Figure 2, in which autophagy gene expression was elevated in fetal tissue as compared with full term tissue. These findings further support the possibility that the premature infant may be susceptible to NEC in part through increased predisposition to the induction of autophagy within the intestinal epithelium, and suggest the physiological relevance of the murine findings.

We next sought to determine whether TLR4 signaling in the intestinal mucosa was required for the induction in autophagy in mice with NEC. To do so, we generated mice that selectively lacked TLR4 within enterocytes (strain $TLR4^{\Delta IEC}$) by crossing TLR4-loxp mice with villin-cre mice as we have recently described (26), and then subjected wild-type, $TLR4^{\Delta IEC}$ and $TLR4^{-/-}$ mice to experimental NEC. As shown in Figure 3 **panels D i**, the induction of NEC in $TLR4^{-/-}$ mice did not cause an increase in enterocyte autophagy as determined by confocal microscopy, indicating that TLR4 activation in NEC is required for this response. The requirement for TLR4 signaling in the induction of enterocyte autophagy in NEC was confirmed biochemically, in which the ratio of LC3-II to actin was not increased in $TLR4^{-/-}$ mice after the induction of NEC, despite this ratio being increased in wild-type mice that were induced to develop NEC at the same time (Figure 3 **panel Ei and ii**). Importantly, TLR4 signaling in the intestinal epithelium as opposed to immune cells was required for the development of enterocyte autophagy, as the induction of NEC in

TLR4$^{\Delta IEC}$ mice did not induce enterocyte autophagy, as measured by confocal microscopy (Figure 3D **panel ii**) and biochemically (Figure 3 **panel E**). Taken together, these findings illustrate that TLR4 signaling leads to a corresponding induction of autophagy in enterocytes.

In order to evaluate whether the induction of autophagy was a cause or a consequence of the development of NEC, we next generated mice that specifically lacked Atg7 within the intestinal epithelium, by crossing Atg7-loxp mice with villin-cre mice. This mouse strain - (heretofore designated strain ATG7$^{\Delta IEC}$) – was found to be healthy and fertile, showed normal lifespan, expressed TLR4 at normal levels within the intestinal mucosa, and were protected from the induction of autophagy in enterocytes after the injection of LPS. Moreover, the ATG7$^{\Delta IEC}$ mice did not demonstrate any difference in the frequency or distribution of any of the intestinal epithelial derived lineages or of the extent of enterocyte proliferation within the intestinal crypts, as shown in Supplemental Figure 2. Importantly, ATG7$^{\Delta IEC}$ mice did not show an induction in enterocyte autophagy after exposure to the model of experimental NEC, as demonstrated both by confocal microscopy (Figure 3 **panel Diii**) and SDS-PAGE (Figure 3 **panel E i and ii**).

The induction of autophagy in the intestinal epithelium is required for the pathogenesis of NEC

To directly test whether the induction on autophagy in the intestinal epithelium was required for the development of NEC, we next assessed the severity of NEC that occurred in the newly created ATG7$^{\Delta IEC}$ strain. As shown in Figure 4, ATG7$^{\Delta IEC}$ mice were ignificantly protected from the severity of NEC, as manifest by preservation of the intestinal architecture as revealed by scanning electron microscopy in which wild-type mice with NEC show blunting and destruction of the intestinal villi that were not observed in ATG7$^{\Delta IEC}$ mice (Figure 4 **panel A i–iv**). Moreover, ATG7$^{\Delta IEC}$ mice subjected to experimental NEC showed normal mucosal histology (Figure 4 **panel A v–viii**) and a marked reduction in the extent of intestinal edema and necrosis that is apparent on gross inspection of the small intestine at the time of sacrifice (Figure 4 **panel A ix-xii**). The reduction in NEC severity in ATG7$^{\Delta IEC}$ mice was confirmed by blinded histological score (Figure 4 **panel Di**), and the detection of a reduced expression of CXCL15 (mouse IL-8 homologue) within the intestinal mucosa (Figure 4 **panel D ii**). Further evidence to support the conclusion that autophagy induction is required for NEC development was revealed by the observation that mice treated with the autophagy inducer rapamycin showed increased NEC severity as manifest by increased tissue injury (Figure 4 **panel C ii and D iii**), whereas mice that were administered the autophagy inhibitor choloroquine showed a reduction in the severity of NEC (Figure 4 **panel C iii and D iii**). It is noteworthy that the injection of rapamycin did not attenuate the degree of LPS-induced expression of the pro-inflammatory cytokines IL-1 or IL-6 within the intestinal mucosa, excluding the possibility that rapamycin exerted a broad inhibition in LPS signaling (Figure 4 **panel B**). Taken in aggregate, these findings support the conclusion that the induction of autophagy within the intestinal epithelium is required for the development of NEC. We next sought to determine the mechanisms by which the induction of autophagy could such a deleterious effect on the intestinal mucosa.

TLR4-induced enterocyte autophagy leads to impaired enterocyte migration in vitro

We have identified in a series of studies that TLR4 induction in enterocytes leads to the development of NEC in part through a significant impairment in enterocyte migration, which leads to impaired mucosal healing and persistent mucosal defects (6, 11, 12, 14, 37). However, the mechanisms by which TLR4 activation impairs enterocyte migration remain incompletely understood, although activation of small molecular G-protein RhoA was found to play a role through its ability to increase cell matrix adhesiveness (11, 28). In order to

determine how autophagy induction by TLR4 could lead to NEC, we next considered the possibility that the induction of autophagy by activation of TLR4 could lead to impaired enterocyte migration. To do so, we first evaluated the ability of IEC-6 enterocytes to migrate into a scraped wound under conditions in which autophagy was either activated or inhibited. As is shown in Figure 5 **panels Ai-iv and** quantified in Figure 5 **panel C**, whereas control IEC-6 cells closed a scraped wound within 12 hours, the activation of autophagy using rapamycin significantly inhibited the rate of enterocyte migration. Because rapamycin may have other effects in cells, we next sought to confirm its specificity for autophagy induction, and therefore engineered IEC-6 cells that were deficient in the critical autophagy genes Atg16 or Atg7 by adenoviral delivery of shRNA. As shown in Figure 5 **panel B** and quantified in Figure 5 **panel C**, treatment of Atg7-k/d or Atg16-k/d cells with rapamycin did not impair enterocyte migration. Importantly, both Atg7-k/d and Atg16-k/d cells showed a significantly greater extent of wound closure as compared to wild-type IEC-6 cells (Figure 5 **panel C**), confirming that the induction in autophagy leads to an inhibition in enterocyte migration. (Figure 5 **panel C**). Based upon these findings, we next sought to evaluate whether the impairment of enterocyte migration that occurs in the setting of LPS exposure actually *required* an induction in enterocyte autophagy. To do so, enterocytes were treated with LPS under conditions in which autophagy could not be induced, either through treatment with the autophagy inhibitor chloroquine (Figure 5 **panel A vii-x** and quantified in Figure 5 **panel C**), or through selective knockdown of either Atg7 or Atg16 (Figure 5 **panel B v–vi** and quantified in Figure 5 **panel C**). . In parallel experiments, the knockdown of Atg7 and Atg16 were confirmed by SDS-PAGE in the indicated cell line (Figure 5 **panel D**). As shown, under conditions in which enterocyte autophagy could not be induced, LPS did not impair enterocyte migration. By showing that the extent of wound closure in enterocytes that lack the ability to induce autophagy are not affected by either LPS or rapamycin – both of which induce autophagy as shown above – these findings provide strong confirmation that the induction of autophagy in response to LPS is *required* for the inhibition of enterocyte migration, and illustrate that TLR4-induction of enterocyte autophagy is largely responsible for the impairment in enterocyte migration that occurs after TLR4 activation.

TLR4-induced enterocyte autophagy leads to impaired enterocyte migration in vivo and in the pathogenesis of NEC

We next sought to evaluate whether TLR4 activation inhibits enterocyte migration via the induction of enterocyte autophagy *in vivo*, and if so, to determine the relevance of these findings to the development of NEC. To do so, we injected wither wild type or $ATG7^{\Delta IEC}$ mice with the nucleotide analogue BrDU – which becomes incorporated into dividing enterocytes at the base of the intestinal crypts – and tracked their migration along the crypt-villus axis in the presence or absence of LPS or the induction of NEC. As shown in Figure 6 **panel A** and quantified in Figure 6 **panel C**, wild-type mice that were injected with LPS showed a significant reduction in the extent of migration of BrDU-labelled enterocytes along the crypt-villus axis, consistent with our earlier findings (6, 11). Importantly, the injection of LPS into $ATG7^{\Delta IEC}$ mice showed no impairment in enterocyte migration (Figure 6 **panel A iii-iv** and quantified in **panel C**), confirming that TLR4 activation inhibits enterocyte migration *in vivo* through the induction of autophagy. To assess the relevance of these findings to the pathogenesis of NEC, wild-type mice and $ATG7^{\Delta IEC}$ mice were subjected to experimental NEC and the extent of enterocyte migration was assessed. As shown in Figure 6 **panel B i–ii** and quantified in Figure 6 **panel D**, the induction of NEC in wild-type mice was associated with significantly reduced enterocyte migration along the crypt-villus axis, consistent with our previous studies (6, 11). Importantly however, the induction of NEC in $ATG7^{\Delta IEC}$ mice did not show an impairment in enterocyte migration, in whom the degree of enterocyte migration was similar to that of breast fed controls (Figure

6 **panel B iii-iv** and quantification in **panel D**). It is noteworthy that although both LPS injection (Figure 6 **panel E**) and the induction of NEC (Figure 6 **panel F**) resulted in a decrease in enterocyte proliferation as measured by the expression of the proliferation marker PCNA within the intestinal epithelium – consistent with our prior studies (31) – the deletion of Atg7 from the intestinal epithelium did not reverse the inhibition in enterocyte proliferation, excluding the likelihood that the induction of autophagy in response to TLR4 was exerting protective effects on NEC development by restoring enterocyte proliferation. Taken together, these results demonstrate that TLR4 inhibits enterocyte migration through the induction of autophagy in enterocytes *in vitro* and *in vivo*, and in the pathogenesis of NEC. We next sought to evaluate the molecular mechanisms by which the induction of autophagy could impair enterocyte migration.

TLR4-induced autophagy leads to the activation of Rho-GTPase in enterocytes which is required for the impairment in enterocyte migration

We and others have shown that the inhibition of enterocyte migration in response to LPS occurs via the activation of the small GTP-ase RhoA, which leads to an increase in actin rich stress fibers, filamentous structures that traverse the cytoplasm and anchor the cell to the underlying matrix (11). Given our current findings that TLR4 activation reduced enterocyte migration through the induction of autophagy, we next considered whether the induction in autophagy leads to RhoA activation, and whether such an increase in RhoA activation is *required* for the autophagy-mediated inhibition of enterocyte migration in response to TLR4. As shown in Figure 7 **panel A**, while LPS treatment led to an induction of RhoA in wild-type IEC-6 cells, as assessed using a pull-down assay for rhotekin which binds only to active RhoA (29), LPS did not cause an increase in RhoA activation in autophagy deficient Atg16-k/d cells (Figure 7 **panel A**), indicating that the induction of autophagy was *required* for the activation of RhoA. These findings were confirmed by confocal microscopic evaluation of stress fiber formation in Figure 7 **panel B**, in which although LPS caused an increase in stress fibers in wild-type cells (Figure 7 **panel B ii versus i**), there was no increase in stress fibers upon LPS treatment in Atg16-k/d cells (Figure 7 **panel C ii vs i**), confirming the importance of autophagy induction in mediating the increase in RhoA. Activation of autophagy with rapamycin also resulted in an increase in stress fibers in wild-type IEC-6 cells – consistent with an increase in RhoA activity – that was not seen in autophagy deficient Atg16-k/d cells (Figure 7 B **panel iii versus 7 C panel iii**). In control experiments, transfection of wild-type and Atg16-k/d IEC-6 cells with constitutively active RhoA restored stress fiber formation (Figure 7 **panel B iv** and **Panel C iv**), indicating that the RhoA signaling pathway was otherwise intact, and confirming that activation of RhoA could rescue the formation of stress fibers in autophagy deficient cells. Taken together, these findings illustrate that the induction of autophagy is required for TLR4-induce RhoA activation and stress fiber formation in enterocytes in vitro.

We next sought to evaluate whether the activation of RhoA in response to autophagy induction was *required* for the inhibition of enterocyte migration by TLR4. To do so, autophagy-deficient Atg7-k/d and Atg16-k/d IEC-6 cells were transfected with constitutively active RhoA, treated with LPS, and assessed for their ability to migrate into a scraped wound. As shown in Figure 7 **panel D**, in autophagy-deficient cells that were transfected with active RhoA, LPS now significantly inhibited enterocyte migration, indicating that transfection with active RhoA could reverse the phenotype observed in the autophagy-deficient cells. In control experiments, transfection of wild-type IEC-6 cells with constitutively-active RhoA had minimal effects on enterocyte migration in the absence of LPS treatment (Figure 7 **panel D**). Taken together, these findings illustrate that TLR4-induced autophagy leads to an inhibition in enterocyte migration in vitro through the

activation of RhoA and increased stress fibers, and identify a novel paradigm explaining the effects of autophagy on enterocyte migration in the setting or TLR4 activation.

Discussion

We now demonstrate that the development of NEC requires a TLR4-dependent increase in autophagy within the intestinal epithelium, and moreover, using conditional knockout mice that specifically lack Atg7 within the intestinal epithelium, we provide evidence that the increase in autophagy is *required* for the development of this disease. And while previous authors have recently described that autophagy is induced in the intestine of animals with NEC (38), the current findings extend those prior observations by identifying that the induction in autophagy within the intestinal epithelium is a *cause* and not a *consequence* of NEC, and also by providing a molecular mechanism to explain how the induction of autophagy occurs in NEC (namely via TLR4 signaling) and how the induction of autophagy leads to NEC (namely via inhibition of enterocyte migration). It is noteworthy that while the premature infant tissue (i.e. fetal tissue) had increased expression of autophagy genes, this was insufficient to cause spontaneous disease; rather, a second hit in the form of TLR4 activation was required, which resulted in impaired migration and the development of NEC.

The current findings represent a marked departure from prevailing thinking in the autophagy field regarding the physiological role of autophagy within cells, which has been chiefly viewed as a response to stress aimed at recycling damaged organelles (39). While previous authors have shown that TLR4 signaling can induce autophagy in leukocytes which can positively regulate microbial clearance and NFkB signaling (15, 40–42), the current studies are unique in that we now identify a role for TLR4-induced autophagy in the regulation of the cytoskeleton and cell migration, and provide the first description of TLR4-induced autophagy specifically within the intestinal epithelium. We readily acknowledge that the current findings do not permit us to determine whether other TLR ligands could activate autophagy with similar versus opposing effects on cell migration, nor whether factors that have been identified to limit TLR4 signaling in the intestinal epithelium – including amniotic fluid-derived epidermal growth factor (33) and intracellular heat shock protein 70 (27) – could also limit TLR4-induced autophagy. However, it is clear that the current findings extend our knowledge of the physiological role that autophagy can serve within cells and tissues, and that the induction of TLR4-induced autophagy is critical in the pathogenesis of NEC via effects on enterocyte migration.

It is interesting to speculate on how the current findings could fit within the prevailing notion that autophagy represents a cell survival role to offset the induction of cell death pathways via apoptosis (43). We now posit that in the initial phases of the development of NEC, such as may occur during a brief hypoxic episode within the intestine of the stressed, preterm infant, the induction of autophagy in enterocytes that is induced by early TLR4 signaling events may actually have a primarily protective role. We further speculate that ongoing TLR4 activation – as would occur in the setting of intestinal colonization within the neonatal intensive care unit – and within the premature intestine in which the expression of critical autophagy genes is significantly increased (see Figure 2), an exaggerated degree of autophagy would occur, which could then readily serve not a protective but rather a primarily pathophysiological role. These dichotomous roles for autophagy within cells suggests that the development of impaired mucosal healing in NEC may actually represent the failure to down-regulate autophagy – a finding that may also play a role in other inflammatory diseases in which exaggerated autophagy has been implicated (16).

The current findings serve also to distinguish the molecular mechanisms that underlie the pathogenesis of necrotizing enterocolitis – in which autophagy induction serves a causative

role – from the colitis seen in adult inflammatory bowel disease – in which autophagy is largely thought to be protective, as inhibitory mutations in the autophagy gene ATG16L are found in patients with inflammatory bowel disease, and in which genetic deletion of Atg16L1 increased the severity of experimental colitis (19) (20, 44). There are several ways to reconcile these apparent differences. First, TLR4 has a significantly different role in the pathogenesis of colitis as compared with NEC: in inflammatory bowel disease, TLR4 is markedly down-regulated and has a minor pathogenic role(45, 46), while in NEC, which occurs in the newborn period in which the expression of TLR4 within the newborn intestinal mucosa is extremely high, TLR4 plays a causative role through the deleterious effects on intestinal mucosal injury and repair (6, 31). Second, autophagy has been shown to play a significant role in the regulation of paneth cells in inflammatory bowel disease, as hypomorphic ATG16L expression in mice causes severe defects in paneth cell granule content and release (47), while in NEC, a role for paneth cells remains uncertain(48). Thirdly, the pathological features of NEC and IBD are obviously quite different, as NEC is associated with impaired intestinal restitution and the development of necrosis, while IBD is characterized by the influx of inflammatory cells and the presence of transmural inflammation. Fourth, there may be a cell type-specific effect of autophagy on disease pathogenesis, in which for instance autophagy in leukocytes in IBD may be protective while autophagy in epithelial cells could be deleterious leading to NEC. And finally, the current studies reflect the situation within the premature or newborn gut – in which autophagy genes are elevated, while studies in models of colitis are largely restricted to adults. It is likely therefore that the induction of autophagy could effect each of these pathways that differ between NEC and IBD, and that the timing and mechanisms by which autophagy is induced within the intestine of the premature versus the adult gut would have substantially different effects.

In summary, we now show that TLR4-induced autophagy plays a critical step in the pathogenesis of NEC, which occurs through the negative regulation of enterocyte migration. Based upon these findings – which lie in distinction to studies on leukocytes and in adult models of inflammatory bowel disease – we now expand on the known roles of autophagy, which has previously been viewed to serve a largely cell protective function. These results also provide novel insights into the effects of TLR4 activation within enterocytes, provide novel mechanistic insights into the pathogenesis of necrotizing enterocolitis, and suggest new therapeutic approaches based upon the regulation of autophagy for this devastating disease.

Supplementary Material

Refer to Web version on PubMed Central for supplementary material.

Acknowledgments

The authors gratefully acknowledge the insights of Dr. David Perlmutter, Children's Hospital of Pittsburgh, in the planning of the current studies. We also acknowledge the creative insights and expertise of Dr. Shipan Dai in the early phases of the current experiments.

DJH is supported by R01GM078238 and RO1DK08752 from the National Institutes of Health. AA is supported by F30DK085930 from the National Institute of Diabetes and Digestive and Kidney Diseases (NIDDK) of the National Institutes of Health.

References

1. Llanos AR, Moss ME, Pinzon MC, Dye T, Sinkin RA, Kendig JW. Epidemiology of neonatal necrotising enterocolitis: a population-based study. Paediatr Perinat Epidemiol. 2002; 16:342–349. [PubMed: 12445151]

2. Neu J, Walker WA. Necrotizing enterocolitis. N Engl J Med. 2011; 363:255–264. [PubMed: 21247316]
3. Grave GD, Nelson SA, Walker WA, Moss RL, Dvorak B, Hamilton FA, Higgins R, Raju TN. New therapies and preventive approaches for necrotizing enterocolitis: report of a research planning workshop. Pediatr Res. 2007; 62:510–514. [PubMed: 17667844]
4. Dominguez KM, Moss RL. Necrotizing enterocolitis. Clin Perinatol. 2012; 39:387–401. [PubMed: 22682387]
5. Caplan MS. Neonatal necrotizing enterocolitis. Introduction. Semin Perinatol. 2008; 32:69. [PubMed: 18346529]
6. Leaphart CL, Cavallo JC, Gribar SC, Cetin S, Li J, Branca MF, Dubowski TD, Sodhi CP, Hackam DJ. A critical role for TLR4 in the pathogenesis of necrotizing enterocolitis by modulating intestinal injury and repair. J. Immunol. 2007; 179:4808–4820. [PubMed: 17878380]
7. Nanthakumar N, Meng D, Goldstein AM, Zhu W, Lu L, Uauy R, Llanos A, Claud EC, Walker WA. The mechanism of excessive intestinal inflammation in necrotizing enterocolitis: an immature innate immune response. PLoS One. 2011; 6:e17776. [PubMed: 21445298]
8. Wolfs TG, Derikx JP, CM H, Vanderlocht J, Driessen A, de Bruïne AP, Bevins CL, Lasitschka F, Gassler N, van Gemert WG, Buurman WA. Localization of the lipopolysaccharide recognition complex in the human healthy and inflamed premature and adult gut. Inflamm Bowel Dis. 2010; 16:68–75. [PubMed: 20014022]
9. Jilling T, Simon D, Lu J, Meng FJ, Li D, Schy R, Thomson RB, Soliman A, Arditi M, Caplan MS. The roles of bacteria and TLR4 in rat and murine models of necrotizing enterocolitis. J Immunol. 2006; 177:3273–3282. [PubMed: 16920968]
10. Gribar SC, A. R, Sodhi CP, Hackam DJ. The role of epithelial Toll-like receptor signaling in the pathogenesis of intestinal inflammation. J Leukoc Biol. 2008; 83:493–498. [PubMed: 18160540]
11. Cetin S, Ford HR, Sysko LR, Agarwal C, Wang J, Neal MD, Baty C, Apodaca G, Hackam DJ. Endotoxin inhibits intestinal epithelial restitution through activation of Rho-GTPase and increased focal adhesions. J Biol Chem. 2004; 279:24592–24600. [PubMed: 15169791]
12. Qureshi FG, Leaphart C, Cetin S, Li J, Grishin A, Watkins S, Ford HR, Hackam DJ. Increased expression and function of integrins in enterocytes by endotoxin impairs epithelial restitution. Gastroenterology. 2005; 128:1012–1022. [PubMed: 15825082]
13. Feng J, Besner GE. Heparin-binding epidermal growth factor-like growth factor promotes enterocyte migration and proliferation in neonatal rats with necrotizing enterocolitis. J Pediatr Surg. 2007; 42:214–220. [PubMed: 17208569]
14. Afrazi A, Sodhi CP, Richardson W, Neal M, Good M, Siggers R, Hackam DJ. New insights into the pathogenesis and treatment of necrotizing enterocolitis: toll-like receptors and beyond. Pediatr Res. 2011; 69:183–188. [PubMed: 21135755]
15. Sanjuan MA, Dillon CP, Tait SW, Moshiach S, Dorsey F, Connell S, Komatsu M, Tanaka K, Cleveland JL, Withoff S, Green DR. Toll-like receptor signalling in macrophages links the autophagy pathway to phagocytosis. Nature. 2007; 450:1253–1257. [PubMed: 18097414]
16. Levine B, Kroemer G. Autophagy in the pathogenesis of disease. Cell. 2008; 132:27–42. [PubMed: 18191218]
17. Klionsky DJ, Baehrecke EH, Brumell JH, Chu CT, Codogno P, Cuervo AM, Debnath J, Deretic V, Elazar Z, Eskelinen EL, Finkbeiner S, Fueyo-Margareto J, Gewirtz D, Jaattela M, Kroemer G, Levine B, Melia TJ, Mizushima N, Rubinsztein DC, Simonsen A, Thorburn A, Thumm M, Tooze SA. A comprehensive glossary of autophagy-related molecules and processes (2nd edition). Autophagy. 2011; 7:1273–1294. [PubMed: 21997368]
18. Levine B, Klionsky DJ. Development by self-digestion: molecular mechanisms and biological functions of autophagy. Dev Cell. 2004; 6:463–477. [PubMed: 15068787]
19. Rioux JD, Xavier RJ, Taylor KD, Silverberg MS, Goyette P, Huett A, Green T, Kuballa P, Barmada MM, Datta LW, Shugart YY, Griffiths AM, Targan SR, Ippoliti AF, Bernard EJ, Mei L, Nicolae DL, Regueiro M, Schumm LP, Steinhart AH, Rotter JI, Duerr RH, Cho JH, Daly MJ, Brant SR. Genome-wide association study identifies new susceptibility loci for Crohn disease and implicates autophagy in disease pathogenesis. Nat Genet. 2007; 39:596–604. [PubMed: 17435756]

20. Saitoh T, Fujita N, Jang MH, Uematsu S, Yang BG, Satoh T, Omori H, Noda T, Yamamoto N, Komatsu M, Tanaka K, Kawai T, Tsujimura T, Takeuchi O, Yoshimori T, Akira S. Loss of the autophagy protein Atg16L1 enhances endotoxin-induced IL-1beta production. Nature. 2008; 456:264–268. [PubMed: 18849965]
21. Macintosh RL, Timpson P, Thorburn J, Anderson KI, Thorburn A, Ryan KM. Inhibition of autophagy impairs tumor cell invasion in an organotypic model. Cell Cycle. 2012; 11:2022–2029. [PubMed: 22580450]
22. Du J, Teng RJ, Guan T, Eis A, Kaul S, Konduri GG, Shi Y. Role of autophagy in angiogenesis in aortic endothelial cells. Am J Physiol Cell Physiol. 2012; 302:C383–C391. [PubMed: 22031599]
23. Sun Y, Liu JH, Sui YX, Jin L, Yang Y, Lin SM, Shi H. Beclin1 overexpression inhibitis proliferation, invasion and migration of CaSki cervical cancer cells. Asian Pac J Cancer Prev. 2011; 12:1269–1273. [PubMed: 21875280]
24. Lee SJ, Kim HP, Jin Y, Choi AM, Ryter SW. Beclin 1 deficiency is associated with increased hypoxia-induced angiogenesis. Autophagy. 2011; 7:829–839. [PubMed: 21685724]
25. Richardson WM, Sodhi CP, Russo A, Siggers RH, Afrazi A, Gribar SC, Neal MD, Dai S, Prindle TJ, Branca M, Ma C, Ozolek J, Hackam DJ. Nucleotide-binding Oligomerization Domain-2 Inhibits Toll Like Receptor-4 Signaling in the Intestinal Epithelium. Gastroenterology. 2010; 139:904–917. [PubMed: 20580721]
26. Sodhi CP, Neal MD, Siggers R, Sho S, Ma C, Branca MF, Prindle T Jr, Russo AM, Afrazi A, Good M, Brower-Sinning R, Firek B, Morowitz MJ, Ozolek JA, Gittes GK, Billiar TR, Hackam DJ. Intestinal epithelial Toll-like receptor 4 regulates goblet cell development and is required for necrotizing enterocolitis in mice. Gastroenterology. 2012; 143:708–718. e701–e705. [PubMed: 22796522]
27. Afrazi A, Sodhi CP, Good M, Jia H, Siggers R, Yazji I, Ma C, Neal MD, Prindle T, Grant ZS, Branca MF, Ozolek J, Chang EB, Hackam DJ. Intracellular Heat Shock Protein-70 Negatively Regulates TLR4 Signaling in the Newborn Intestinal Epithelium. J Immunol. 2012; 188:4543–4557. [PubMed: 22461698]
28. Dai S, Sodhi CP, Cetin S, Richardson W, Branca M, Neal MD, Prindle T, Ma C, Shapiro RA, Li B, Wang JH, Hackam DJ. Extracellular high mobility group box1 (HMGB1) inhibits enterocyte migration via activation of toll like receptor 4 and increased cell-matrix adhesiveness. J Biol Chem. 2010; 285:4995–5002. [PubMed: 20007974]
29. Reid T, Furuyashiki T, Ishizaki T, Watanabe G, Watanabe N, Fujisawa K, Morii N, Madaule P, Narumiya S. Rhotekin, a new putative target for Rho bearing homology to a serine/threonine kinase, PKN, and rhophilin in the Rho-binding domain. J Biol Chem. 1996; 271:13556–13560. [PubMed: 8662891]
30. Leaphart CL, Qureshi F, Cetin S, Li J, Dubowski T, Batey C, Beer-Stolz D, Guo F, Murray SA, Hackam DJ. Interferon-[gamma] inhibits intestinal restitution by preventing gap junction communication between enterocytes. Gastroenterology. 2007; 132:2395–2411. [PubMed: 17570214]
31. Sodhi CP, Shi XH, Richardson WM, Grant ZS, Shapiro RA, Prindle TJ, Branca M, Russo A, Gribar SC, Ma C, Hackam DJ. Toll-like Receptor-4 Inhibits Enterocyte Proliferation via Impaired beta-Catenin Signaling in Necrotizing Enterocolitis. Gastroenterology. 2010; 138:185–196. [PubMed: 19786028]
32. Komatsu M, Waguri S, Ueno T, Iwata J, Murata S, Tanida I, Ezaki J, Mizushima N, Ohsumi Y, Uchiyama Y, Kominami E, Tanaka K, Chiba T. Impairment of starvation-induced and constitutive autophagy in Atg7-deficient mice. J Cell Biol. 2005; 169:425–434. [PubMed: 15866887]
33. Good M, Siggers RH, Sodhi CP, Afrazi A, Alkhudari F, Egan CE, Neal MD, Yazji I, Jia H, Lin J, Branca MF, Ma C, Prindle T, Grant Z, Shah S, Slagle D 2nd, Paredes J, Ozolek J, Gittes GK, Hackam DJ. Amniotic fluid inhibits Toll-like receptor 4 signaling in the fetal and neonatal intestinal epithelium. Proc Natl Acad Sci U S A. 2012; 109:11330–11335. [PubMed: 22733781]
34. Lorne E, Zhao X, Zmijewski JW, Liu G, Park YJ, Tsuruta Y, Abraham E. Participation of mammalian target of rapamycin complex 1 in Toll-like receptor 2- and 4-induced neutrophil activation and acute lung injury. Am J Respir Cell Mol Biol. 2009; 41:237–245. [PubMed: 19131641]

35. Jiang M, Liu K, Luo J, Dong Z. Autophagy is a renoprotective mechanism during in vitro hypoxia and in vivo ischemia-reperfusion injury. Am J Pathol. 2010; 176:1181–1192. [PubMed: 20075199]
36. Maiuri MC, Zalckvar E, Kimchi A, Kroemer G. Self-eating and self-killing: crosstalk between autophagy and apoptosis. Nat Rev Mol Cell Biol. 2007; 8:741–752. [PubMed: 17717517]
37. Mi Q, Swigon D, Rivière B, Cetin S, Vodovotz Y, Hackam DJ. One-dimensional elastic continuum model of enterocyte layer migration. Biophys J. 2007; 93:3745–3752. [PubMed: 17704181]
38. Maynard AA, Dvorak K, Khailova L, Dobrenen H, Arganbright KM, Halpern MD, Kurundkar AR, Maheshwari A, Dvorak B. Epidermal growth factor reduces autophagy in intestinal epithelium and in the rat model of necrotizing enterocolitis. Am J Physiol Gastrointest Liver Physiol. 2010; 299:G614–G622. [PubMed: 20539009]
39. Jia K, Levine B. Autophagy and longevity: lessons from C. elegans. Adv Exp Med Biol. 2010; 694:47–60. [PubMed: 20886756]
40. Sanjuan MA, Green DR. Eating for good health: linking autophagy and phagocytosis in host defense. Autophagy. 2008; 4:607–611. [PubMed: 18552553]
41. Xu Y, Jagannath C, Liu XD, Sharafkhaneh A, Kolodziejska KE, Eissa NT. Toll-like receptor 4 is a sensor for autophagy associated with innate immunity. Immunity. 2007; 27:135–144. [PubMed: 17658277]
42. Shi CS, Shenderov K, Huang NN, Kabat J, Abu-Asab M, Fitzgerald KA, Sher A, Kehrl JH. Activation of autophagy by inflammatory signals limits IL-1beta production by targeting ubiquitinated inflammasomes for destruction. Nat Immunol. 2012; 13:255–263. [PubMed: 22286270]
43. Kang R, Zeh HJ, Lotze MT, Tang D. The Beclin 1 network regulates autophagy and apoptosis. Cell Death Differ. 2011; 18:571–580. [PubMed: 21311563]
44. Hampe J, Franke A, Rosenstiel P, Till A, Teuber M, Huse K, Albrecht M, Mayr G, De La Vega FM, Briggs J, Gunther S, Prescott NJ, Onnie CM, Hasler R, Sipos B, Folsch UR, Lengauer T, Platzer M, Mathew CG, Krawczak M, Schreiber S. A genome-wide association scan of nonsynonymous SNPs identifies a susceptibility variant for Crohn disease in ATG16L1. Nat Genet. 2007; 39:207–211. [PubMed: 17200669]
45. Santaolalla R, Abreu MT. Innate immunity in the small intestine. Curr Opin Gastroenterol. 2012; 28:124–129. [PubMed: 22241076]
46. Cario E, Podolsky DK. Differential alteration in intestinal epithelial cell expression of toll-like receptor 3 (TLR3) and TLR4 in inflammatory bowel disease. Infect Immun. 2000; 68:7010–7017. [PubMed: 11083826]
47. Cadwell K, Liu JY, Brown SL, Miyoshi H, Loh J, Lennerz JK, Kishi C, Kc W, Carrero JA, Hunt S, Stone CD, Brunt EM, Xavier RJ, Sleckman BP, Li E, Mizushima N, Stappenbeck TS, Virgin HWt. A key role for autophagy and the autophagy gene Atg16l1 in mouse and human intestinal Paneth cells. Nature. 2008; 456:259–263. [PubMed: 18849966]
48. Sherman MP, Bennett SH, Hwang FF, Sherman J, Bevins CL. Paneth cells and antibacterial host defense in neonatal small intestine. Infect Immun. 2005; 73:6143–6146. [PubMed: 16113336]

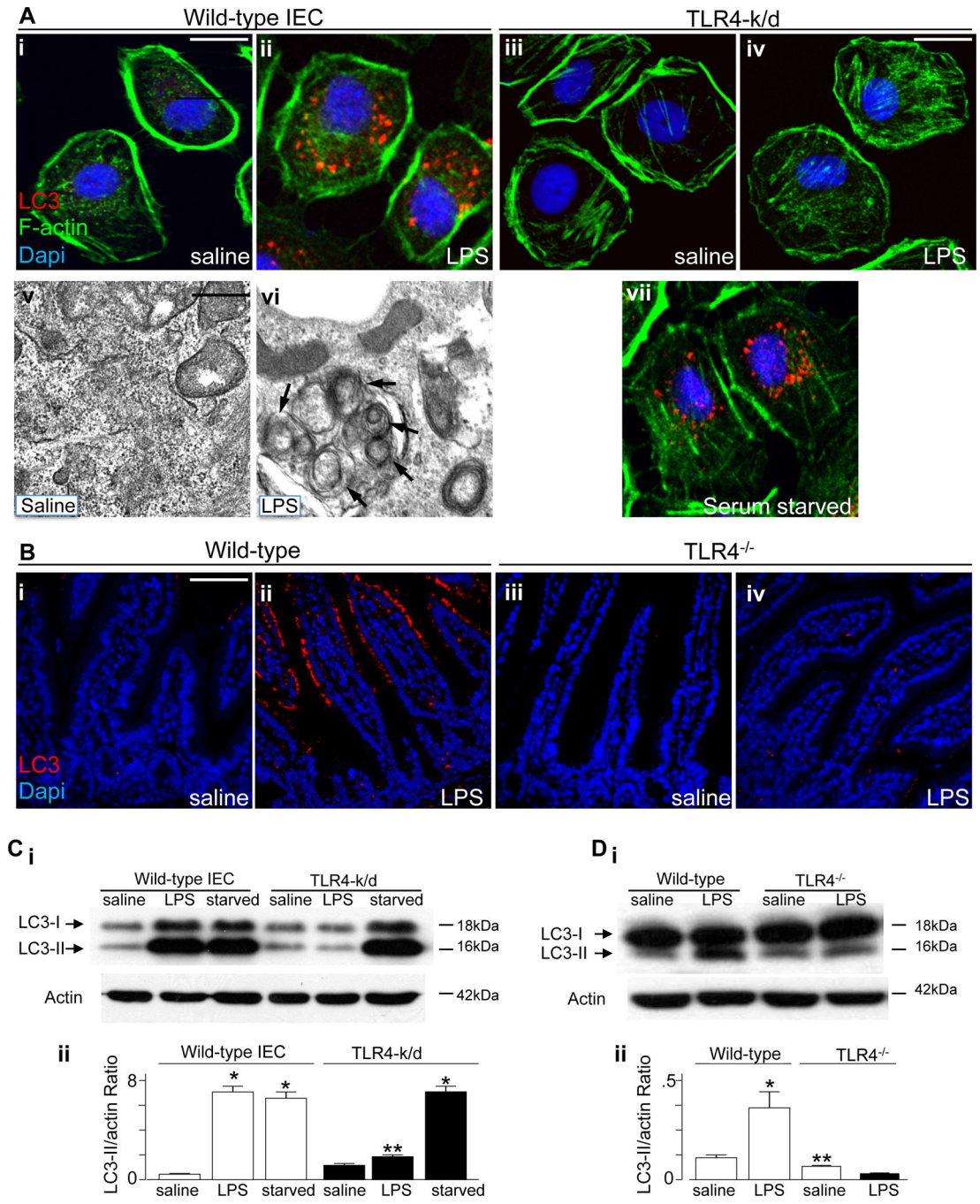

Figure 1. TLR4 induces autophagy in intestinal epithelial cells in vitro and in vivo

A: Representative confocal (**panels i–iv and vii**) and transmission electron (**panels v–vi**) micrographs showing autophagosomes within IEC-6 cells under after treatment with saline, LPS or serum starvation as noted in the bottom right corner of each panel. Red=LC3, green=f-actin, blue=DAPI. Size bar = 10μm in confocal images, 10nm in electron microscopic images. Arrows show double-membrane autophagosomes. **B:** Representative confocal micrographs showing the terminal ileum of newborn wild-type (**panels i–ii)** or TLR4$^{-/-}$ mice (**panels iii-iv**) after treatment with saline or LPS as shown, and stained for LC3 (red) and DAPI (blue). **C–D:** SDS-PAGE showing the expression of LC3-I and LC3-II

in either wild-type or TLR4-k/d IEC-6 cells (**panel C**) or mucosal scrapings from wild-type or $TLR4^{-/-}$ mice (**panel D**); blots were stripped and re-probed for f-actin. Quantification of LC3-II to actin expression ratio is shown in **Cii and Dii**. *$p<0.05$ vs saline; **$p<0.05$ vs LPS-treated wild-type. Representative of 3 separate experiments. Size bar = 1μm.

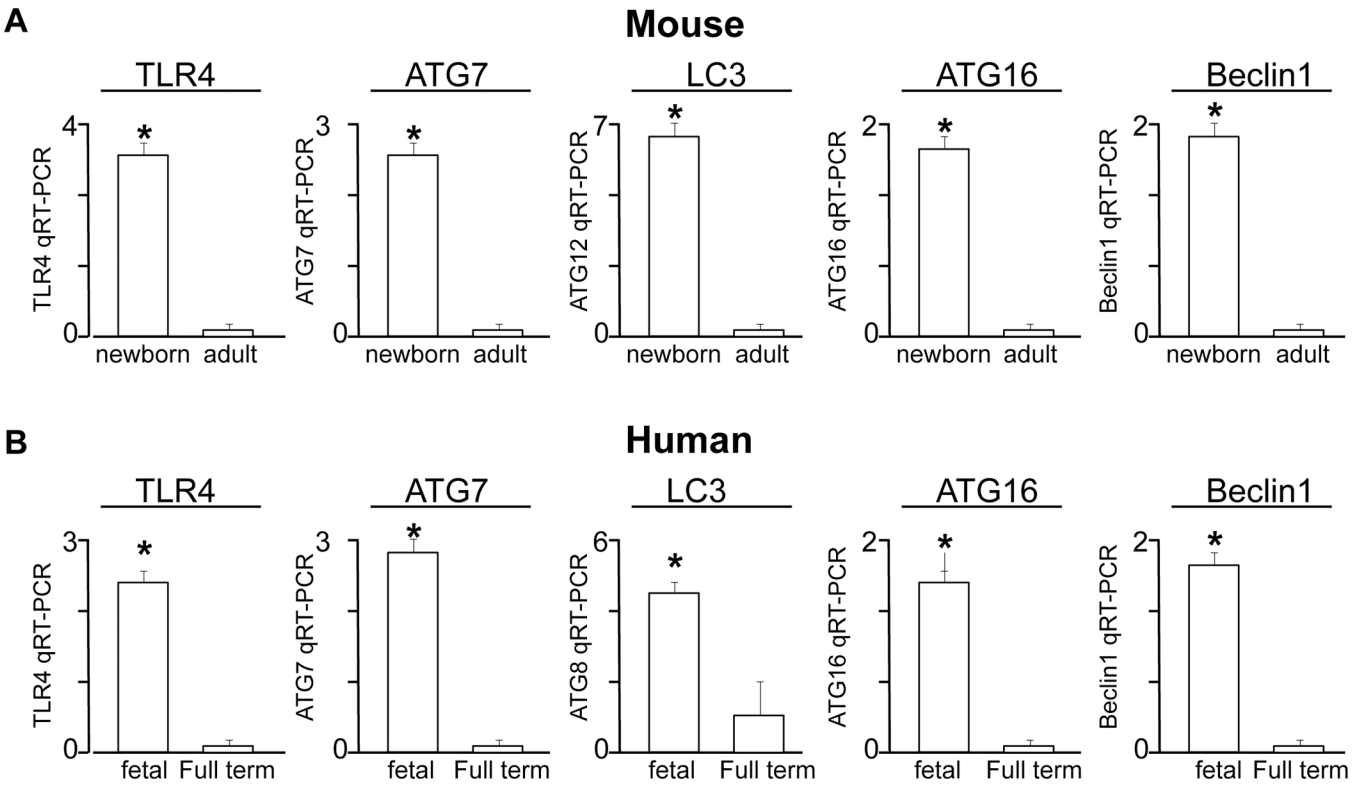

Figure 2. Autophagy genes are increased in the premature versus full term intestine in both mice and humans

qRT-PCR of the indicated gene in the intestine of the newborn versus adult mouse (**A**) and the fetal versus full term intestine of the human (**B**). Representative of at least 3 separate samples per group; *p>0.05 between groups.

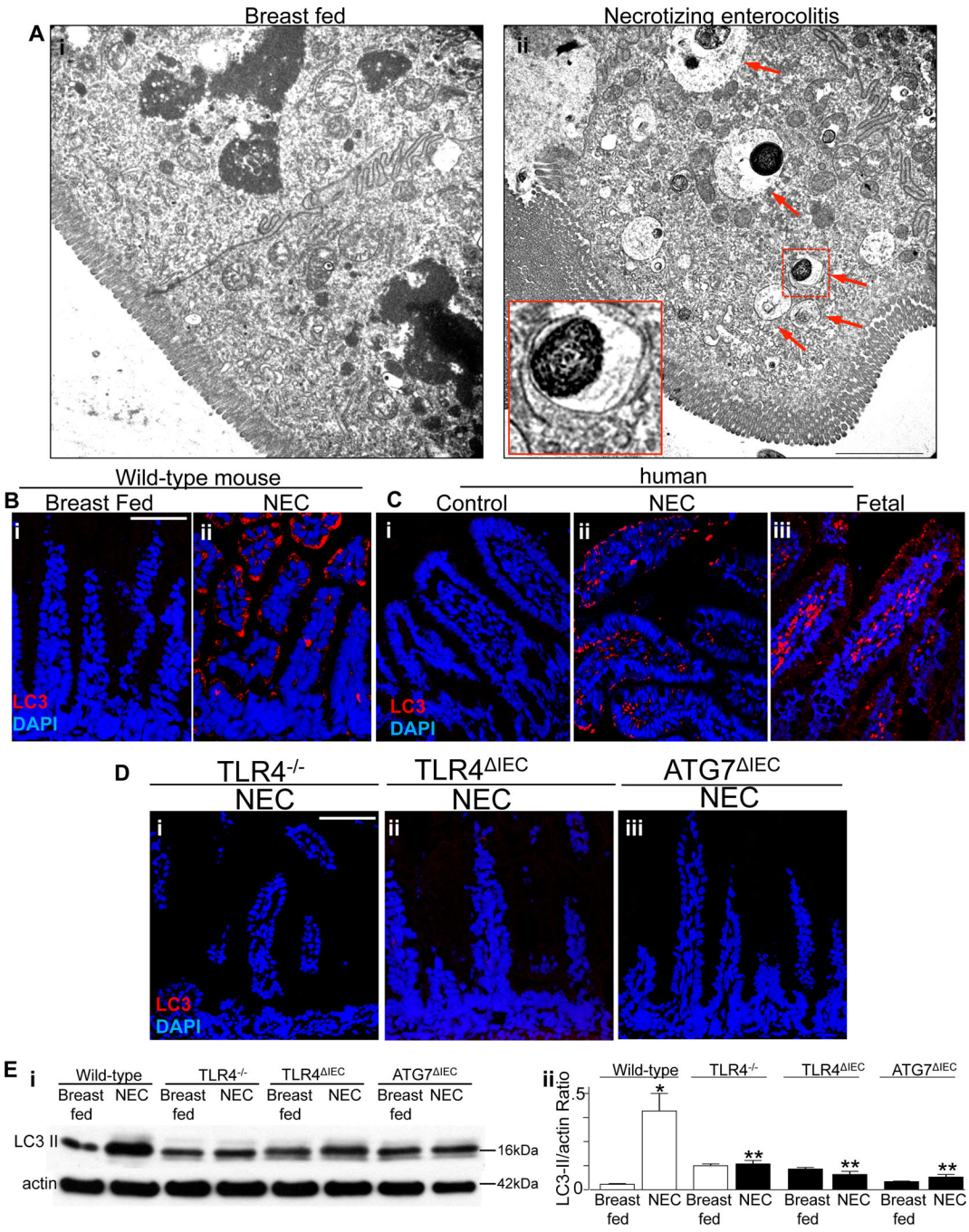

Figure 3. Enterocyte autophagy occurs in mice and humans with NEC, and in mice requires TLR4 activation

A: Representative transmission electron micrographs obtained from the terminal ileum of mice that were breast fed (**i**) or induced to develop NEC (**ii**); arrows in **ii** shows double-membrane autophagosomes; inset shows a representative double-membrane bound autophagosome at 3.2 × magnification corresponding to the dotted line in **ii. B–D:** Representative confocal micrographs showing the expression of the autophagosome marker LC3 (red) and DAPI (blue) in either wild-type mice (**B i–ii**), human tissue (**C i–ii**) or mice that were globally deficient in TLR4 (**D i**), selectively lacking TLR4 within the intestinal epithelium (**D ii**), or selectively lacking Atg7 within the intestinal epithelium (**D iii**); mouse

or human tissue was obtained from either control (breast fed, **B i, C i**) or NEC (**B ii, C ii, D i–iii**). Representative of at least 3 separate experiments. Size bar = 10μm **Ei:** SDS-PAGE showing the expression of LC3-II in the mucosal scrapings from mice of the indicated strain that were either breast fed or subjected to experimental NEC as indicated. Blots were stripped and re-probed for f-actin. Quantification of LC3-II to actin expression ratio is shown in **Eii**. *$p<0.05$ vs breast fed; **$p<0.05$ vs wild-type NEC. Representative of 3 separate experiments.

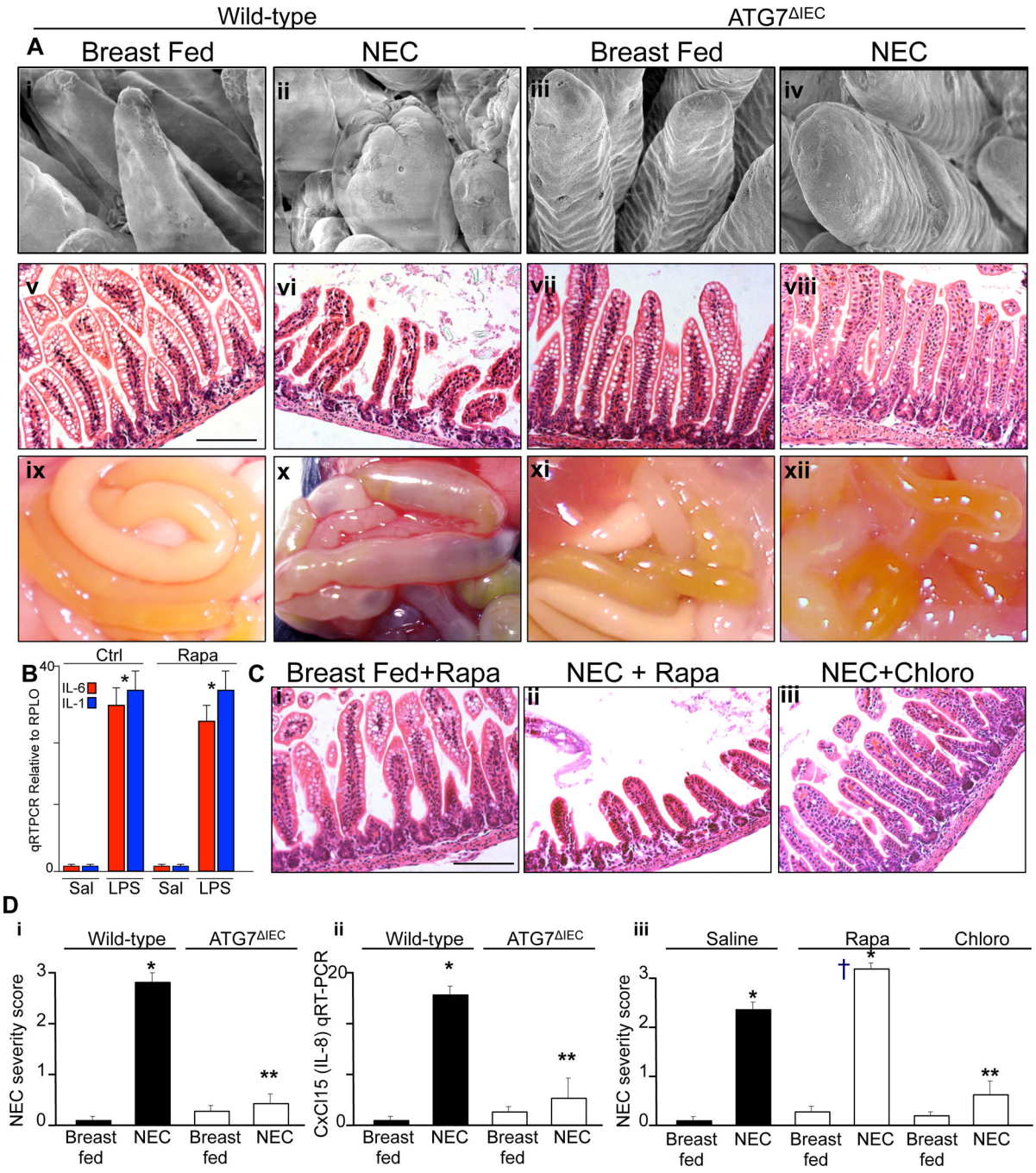

Figure 4. The induction of autophagy in the intestinal epithelium is required for the pathogenesis of NEC

A: Representative micrographs showing scanning electron microscopy (**i–iv**), H&E staining (**v–viii**), and gross morphology of the intestine at the time of euthanasia (**ix-xii**) in either wild-type or ATG7$^{\Delta IEC}$ mice that were either breast fed or subjected to experimental NEC as indicated. Size bar=100μm. **B**. qRT-PCR relative to RPLO of mucosal scrapings obtained from the terminal ileum of newborn mice injected with LPS for 6h (5mg/kg), after pre-injection overnight with rapamycin (5mg/kg); shown are the expression of IL-6 (red bars) and IL-1 (blue bars); *p<0.05 vs saline for each group. **C**: H&E micrographs of the terminal ileum of newborn mice who were either breast fed and subjected to rapamycin (**i**), or

induced to develop NEC and also subjected to rapamycin (**ii**) or chloroquine (**iii**). Size bar=100μm. **D**: Quantification of NEC severity score (**i** and **iii**) and expression of CxCl15 (**ii**) in the terminal ileum of mice that were either breast fed or induced to develop NEC under the strain (**i** and **ii**) or treatment condition (**iii**) indicated. Representative of 3 separate experiments with at least 5 mice per group. *$p<0.05$ vs breast fed; **$p<0.005$ vs NEC-chloro vs NEC-saline; †$p<0.05$ NEC-rapamycin vs NEC-saline, representative of 3 separate experiments.

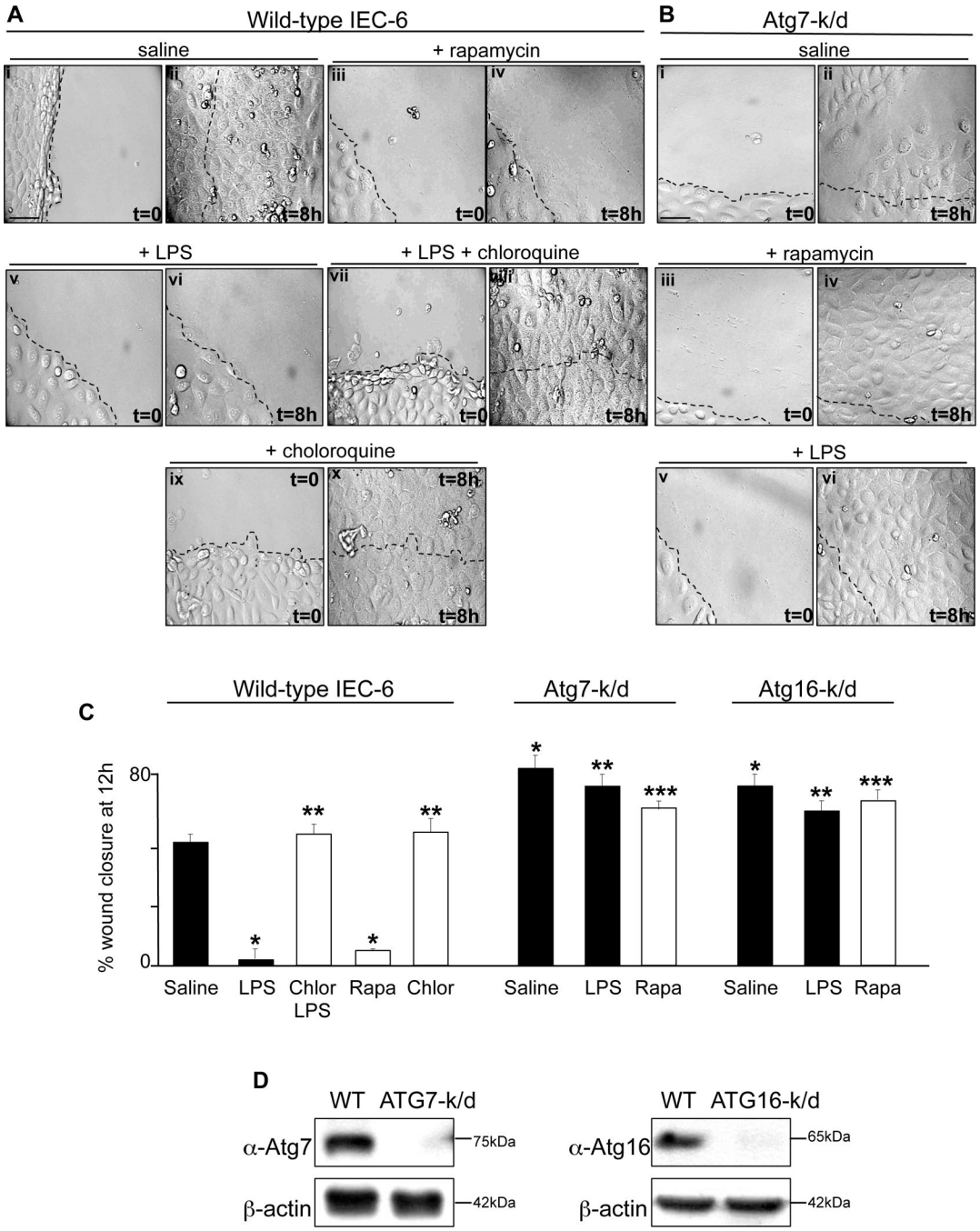

Figure 5. TLR4-induced enterocyte autophagy leads to impaired enterocyte migration in vitro

A–B: Representative paired confocal micrographs from wound scrape assays that are obtained at t=0 at the time of scrape (**Ai, Aiii, Av, Avii, Aix** and **Bi, Biii, Bv**) or at a point 8 hours later (**Aii, Aiv, Avi, Aviii, Ax** and **Bii, Biv, Bvi**) in wild-type (**A**) or Atg7-k/d (**B**) IEC-6 cells that had been treated with either saline (**Ai-ii, Bi-ii**), rapamycin (**Aiii-iv, Biii-iv**), LPS (**Av-vi, Bv-vi**), LPS+chloroquine (**Avii-viii**), or chloroquine alone (**Aix-x**). All panels were obtained at same magnification, size bar=10μm, dashed line indicates the starting point of cell migration at which the scrape was performed **C**: Quantification of migration of wild-type, Atg7-k/d or Atg16-k/d IEC-6 cells expressed as a percent of wound closure, under the

indicated conditions. *p<0.05 vs saline treated wild-type IEC-6 cells; **p<0.05 vs LPS treated wild-type IEC-6 cells; ***p<0.05 vs rapamycin treated wild-type IEC-6 cells. Representative of 4 separate experiments. **D**. SDS-PAGE of Atg7-k/d and ATG16-k/d IEC-6 cells which were immunoblotted using antibodies against Atg7 and Atg16, respectively, as indicated. Blots were stripped and re-probed with antibodies against β-actin. Representative of 3 separate experiments.

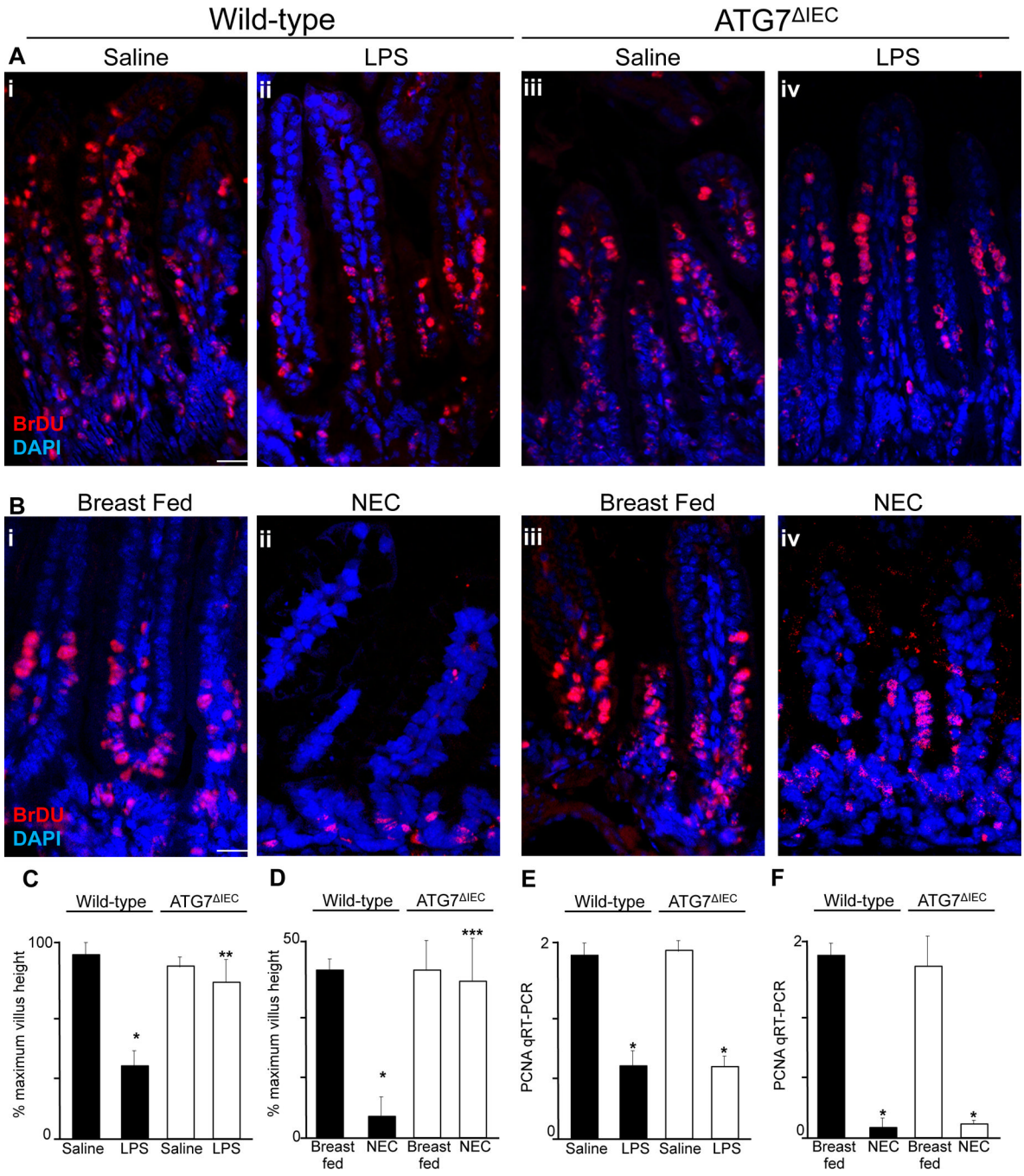

Figure 6. TLR4-induced enterocyte autophagy leads to impaired enterocyte migration in vivo and in the pathogenesis of NEC

A–B: Representative confocal micrographs obtained from the terminal ileum of wild-type (**Ai-ii, Bi-ii**) and ATG7$^{\Delta IEC}$ (**Aiii-iv, Biii-iv**) mice that were either injected with either saline (**Ai, Aiii**), or LPS (**Aii, Aiv**) or were either breast fed (**Bi, Biii**) or induced to develop NEC (**Bii, Biv**) 36h after injection with BrDU, then stained for BrDU (red) and DAPI (blue). Size bar=10μm. **C–D:** Quantification of enterocyte migration along the crypt-villus axis expressed as a percentage of maximum villus height obtained in wild-type or ATG7$^{\Delta IEC}$ mice as indicated; *p<0.05 vs saline or breast fed controls in wild-type mice; **p<0.05 vs LPS treated wild-type mice; ***p<0.05 vs NEC-treated wild-type mice. Representative of 3

separate experiments. Quantification based upon over 100 fields with over 10 villi per field. **E–F:** qRT-PCR showing the expression of the proliferation marker PCNA in the intestinal mucosa in the strain indicated after either injection of LPS (1mg/kg, 12h) or saline (**E**) or after the induction of NEC (**F**); *$p<0.05$ vs either saline or breast fed groups in the paired strain as indicated.

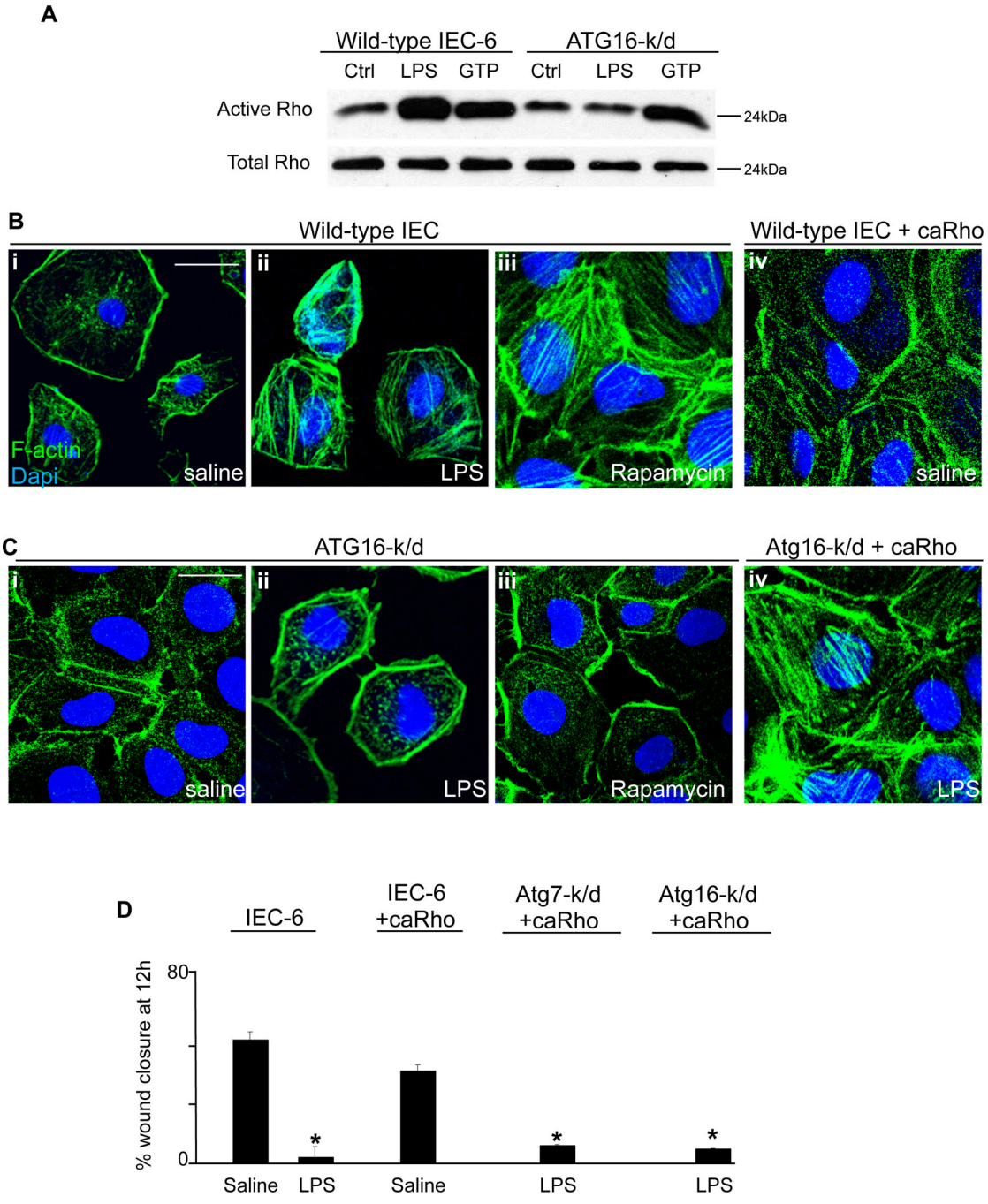

Figure 7. TLR4-induced autophagy leads to the activation of Rho-GTPase in enterocytes which is required for the impairment in enterocyte migration

A: SDS-PAGE in which wild-type and Atg16-k/d IEC-6 cell lysates were blotted with antibodies to GST beads after pull-down with rhotekin-bound beads which binds to active RhoA. Blots were then probed with antibodies to total RhoA (lower bands). **B–C:** Confocal micrographs of wild-type IEC-6 cells (panels **Bi-iii**), IEC-6 cells that were virally transduced with constitutively active RhoA (**Biv**), Atg16-k/d cells (**Ci-iii**) or Atg16-k/d cells that were subsequently virally transduced with constitutively active RhoA (**Civ**) that were stained for actin stress fibers with phalloidin (green) and DAPI (blue) after treatment with either saline or LPS as indicated. Size bar=10μm. **D**: Quantification of migration of wild-type or

transfected IEC-6 cells under the treatment conditions indicated as expressed as a percentage of wound closure as indicated. Representative of 3 separate experiments. *$p<0.05$ vs saline treated wild-type cells.